第21卷 第3期　　广州大学学报(自然科学版)　　Vol. 21 No. 3
2022年 9月　　Journal of Guangzhou University(Natural Science Edition)　　September 2022

文章编号:1671-4229(2022)03-0055-12

有反铁磁近邻作用的海森堡铁磁长程作用自旋链的低温性质的修正自旋波理论研究

张修志，陈　渊*
(广州大学 物理与材料科学学院，广东 广州　510006)

摘　要： 文章将修正的自旋波理论应用于研究具有铁磁长程相互作用 J_0/r^p 和反铁磁近邻相互作用 J 的海森堡铁磁链.通过限制总磁化强度为零,利用自洽方法得到了系统的自旋波热力学.结果表明,铁磁长程相互作用和反铁磁近邻相互作用对系统的低温性质有很大的影响.比热 C 和比热系数 $C/T^{1/(p-1)}$ 均呈现受 p 与 J 诱导的低温峰值行为,而磁化率系数 χT^2 显示了有一最小值,且受 p 与 J 诱导的低温行为.当 $J=0$ 时,且在大 p 极限下,本文的结果与精确贝特方案的结果和量子蒙特卡罗数据吻合得很好.

关键词： 修正自旋波理论；海森堡铁磁链；长程相互作用；最近邻相互作用
中图分类号： O 482.52　　**文献标志码：** A

Modified spin wave theory applied to the low-temperature properties of ferromagnetic long-range interacting spin chain with the antiferromagnetic nearest-neighbor interaction

*ZHANG Xiu-zhi, CHEN Yuan**
(School of Physics and Materials Science, Guangzhou University, Guangzhou 510006, China)

Abstract: In this paper, the modified spin-wave theory is applied to the Heisenberg ferromagnetic chain with the ferromagnetic long-range interaction J_0/r^p and antiferromagnetic nearest-neighbor interaction J. The spin-wave thermodynamics of the system are obtained within the self-consistent method by constraining the total magnetization to be zero. It is shown that the ferromagnetic long-range and antiferromagnetic nearest-neighbor interactions have great influence on the low-temperature properties of the system. At low temperatures, it is found that the specific heat C exhibits the temperature-dependent peak behavior which is induced by p and J, along with the specific heat coefficient $C/T^{1/(p-1)}$; while the susceptibility coefficient χT^2 shows the low-temperature behavior with a minimum induced by p and J. For $J=0$ and in the large-p limit, our results agree well with the exact Bethe ansatz results and the quantum Monte Carlo data.

Key words: modified spin wave theory; Heisenberg ferromagnetic chain; long-range interaction; nearest-neighbor interaction
CLC number: O 482.52　　**Document code:** A

Foundation item: Supported by National Natural Science Foundation of China (11604059); Science and Technology Program of Guangzhou, China (202002030274)

Biography: ZHANG Xiu-zhi (1982—), male, postgraduate. E-mail: 415759018@qq.com
* Corresponding author. E-mail: chenyuan@gzhu.edu.cn

Citation: ZHANG Xiu-zhi, CHEN Yuan. Modified spin wave theory applied to the low-temperature properties of ferromagnetic long-range interacting spin chain with the antiferromagnetic nearest-neighbor interaction[J]. Journal of Guangzhou University(Natural Science Edition), 2022, 21(3):55-66.

0 Introduction

The standard spin-wave theory[1-3] is known as a powerful method in the study of the low-temperature thermodynamics of magnetic systems which can be described by the Heisenberg model. It still gives a boost to further theoretical and experimental explorations[4-8] of Heisenberg magnets. However, when the space dimension is lower than three, the traditional spin-wave theory can't work well, and gives no quantitative information on the thermodynamic physical properties in the paramagnetic phase. This is because there has no long-range order in the paramagnetic phase in low-dimensional isotropic magnetic systems[9]. The spin-wave theory can't cure the thermodynamic divergences which come from the absence of long-range order in the paramagnetic phase.

Fortunately, these thermodynamic divergences can be suppressed by use of Takahashi's idea[10], which is to modify the traditional ferromagnetic spin-wave theory by constraining the total magnetization be zero. As a consequence, Takahashi[10] succeeded in deriving the correct low-temperature properties which are in excellent agreement with Bethe ansatz (BA) results in one dimension. His idea had been extended to many different kinds of low-dimensional magnets, such as the antiferromagnets[11-14], ferrimagnets[15-18], frustrated magnets[19-23], planar magnets[24-26], and spin-phonon coupling systems[27-29]. Based on Takahashi's idea, the modified spin-wave theory gives the good description for inelastic-neutron-scattering measurements of the high-temperature-superconductor-parent antiferromagnet La_2CuO_4[14], and the existence of magnetically ordered phases of magnetic organic salts[30], and the quantum spin-liquid behavior of ultracold bosons on an inhomogeneous triangular lattice[31]. The nuclear spin-lattice relaxation time for the molecular cluster $Mn_{12}O_{12}$ acetate[32] and the ferrimagnetic chain compound $NiCu(C_7H_6N_2O_6)(H_2O)_3 \cdot 2H_2O$[33] is explained well in terms of the modified spin-wave theory. Modified spin-wave analysis of the delta chain with competing ferro- and antiferromagnetic interactions[34] is in agreement with the experimental results of the synthesized cyclic compound $Fe_{10}Gd_{10}$.

In this paper, along the same lines, we formulate a theory for the one-dimensional ferromagnetic long-range interacting Heisenberg model with the antiferromagnetic nearest-neighbor interaction (ANNI). The ferromagnetic long-range interaction (FLRI) considered in this paper decays as J_0/r^p with r being the distance between lattice sites. For the case without the ANNI, the FLRI effect was investigated for the low-temperature and critical properties of the one- and two-dimensional quantum Heisenberg ferromagnets by using modified spin-wave theory[35] and Green's function method[36]. Quantum criticality induced by the transverse magnetic field was obtained in the competition between the anisotropic FLRI (in which its isotropic part decays as r^{-3}) and nearest-neighbor ferromagnetic exchange interactions in the ferromagnetic chain within the traditional spin-wave theory and renormalization group method[37]. Exploiting the renormalization group theory and numerical density matrix renormalization group analysis, continuous symmetry breaking in the Heisenberg chain was shown[38] to take place in the presence of the FLRI without the ANNI. For the ferromagnetic chain in coexistence of the FLRI and ANNI, however, little is known about the thermodynamic properties and critical phenomena. Its corresponding one-dimensional antiferromagnetic cases had been studied for the ground-state properties affected by both the ANNI and antiferromagnetic long-range interactions within Lanczos exact diagonalization[39] and density matrix renormalization group[40]. The recent experimental studies of the perovskites suggested that $Pr_{0.5}Sr_{0.5}MnO_3$[41] and $Pr_{0.5}Sr_{0.5}CoO_{3-x}$[42] as well as Y_2CoMnO_6[43] can be described by the Heisenberg models with both the FLRI (decays as $r^{-3.252}$ in two dimensions[41] and $r^{-4.5}$ in three dimensions[42-43]) and the ANNI. Those theoretical and experimental studies show that the FLRI can lead to the novel magnetic properties. Motivated by the experimental studies, we will consider the magnetic properties which are induced by the competition between the FLRI and ANNI in the ferromagnetic chain. Unlike in the ground state of the one-dimensional ferromagnetic long-range systems without the ANNI[35-38], the ANNI tends to flip the spins and destroys the stability of the ferromagnetic ground state which is kept by the FLRI. In this paper, the scheme to realize Takahashi's idea is a self-consistent method, which can cure the usual thermal divergences by introducing a Lagrangian multiplier in the Hamiltonian to keep zero magnetization. In the frame of spin-wave theory within Takahashi's idea, how the FLRI and the ANNI affect the low-temperature behaviors of the thermodynamic properties is the aim in our paper.

This paper is organized in the following manner. In Section 1, we rewrite the Hamiltonian by using the modified spin-wave theory within the self-consistent method. Then we obtain the analytical expression of the thermodynamic properties (such as the critical temperature, internal energy, specific heat, and susceptibility) as a function of the temperature, the FLRI and the ANNI. Numerical results and some discussions are displayed in Section 2. A brief conclusion is exhibited in Section 3.

1 Model

In this section, the modified spin-wave method will be used to study the thermodynamic properties of the quantum Heisenberg chain with the FLRI and ANNI. The Hamiltonian of the system can be described by

$$H = -J_0 \sum_{i,j} \frac{1}{r_{ij}^p} \vec{s}_i \cdot \vec{s}_j + J \sum_{\langle i,j \rangle} \vec{s}_i \cdot \vec{s}_j \tag{1}$$

Here $\vec{s}_i = (S_i^x, S_i^y, S_i^z)$ stands for the spin S operator with the (x, y, z) components at the ith site. The FLRI has a power-law behavior, which decays as J_0/r_{ij}^p with r_{ij} being the distance between lattice sites i and j. p is the interaction range parameter for the FLRI. J denotes the ANNI. The first sum is over all pairs of spins in the chain. $\langle i, j \rangle$ represents the second summation of the nearest neighbors. The total numbers of the spins is N in the chain.

The FLRI and ANNI in the Hamiltonian (1), which account for the magnetization, are purely electrostatic Coulomb interactions in nature[44]. These two exchange interactions are constructed with completely antisymmetrized wave functions. In Eq. (1), the spin-spin interaction $\vec{s}_i \cdot \vec{s}_j$ acting on the corresponding spin states, simulates the contribution of the exchange matrix elements of the Coulomb interaction. The pole the FLRI plays in the ground state of the system is different from that of the ANNI. The FLRI stabilizes the ferromagnetic ground state. But the ANNI is inherently frustrated, and it can destroy the ferromagnetic long-range order in the ground state.

Two- and three-dimensional versions of the Hamiltonian (1) with the coexistence of the FLRI and ANNI have been experimentally shown to be realized in the perovskites $Pr_{0.5}Sr_{0.5}MnO_3$[41], $Pr_{0.5}Sr_{0.5}CoO_{3-x}$[42] and Y_2CoMnO_6[43]. As pointed out in Ref. [41] in the experimental study on the perovskites, the change in shape and size of the ferromagnetic clusters with temperature around the critical temperature can lead to quasi-one-dimensional perovskites, which may realize the chain Hamiltonian in Eq. (1). The perovskite is an example of the ABX_3 compounds, where A is an alkaline metal ion, B is a magnetic ion, and X is a halogen. These materials are particularly interesting because the ANNI is of the same order of magnitude as the FLRI. In these systems, due to the polarization of the itinerant electrons by interaction with the localized spins at a distance r[44], results in the FLRI between the localized spins of the magnetic ions. The Hamiltonian in Eq. (1) can also be realized in the experimental manipulation of quantum long-range interacting spin chains, which are designed by optical-dipole-force-induced spin-spin interactions in a trapped-ion ferromagnetic Heisenberg chain[45-47]. When the Coulomb interaction is considered as a perturbation to the trapping potential, the FLRI is approximated as a power-law-decay $r-p$ within the frame of the quantum perturbation theory[45-47]. The exponent p of the FLRI corresponds physically to the Coulomb-like interaction for $p=1$, the monopole-dipole interaction for $p=2$, the dipole-dipole interaction for $p=3$, and van de Waals interactions for $p=6$.

As mentioned above, the divergences of the occupation number per site are encountered in the usual spin-wave theory in the disorder phase in one dimension. In order to overcome these divergences, we use Takahashi's idea[10] which constrains the total magnetization to be zero:

$$\sum_i S_i^z = 0 \tag{2}$$

To enhance the Constraint (2), we introduce a Lagrange multiplier λ in the Hamiltonian, then the effective Hamiltonian is given by

$$H_{eff} = -J_0 \sum_{i,j} \frac{1}{r_{ij}^p} \vec{s}_i \cdot \vec{s}_j + J \sum_{\langle i,j \rangle} \vec{s}_i \cdot \vec{s}_j - \lambda \sum_i S_i^z \tag{3}$$

By using the spin raising and lowering operators, $S_i^{\pm} = S_i^x \pm S_i^y$, and making the Holstein-Primakoff transformation[48]

$$S_i^+ = \sqrt{2S - a_i^+ a_i}\, a_i,\ S_i^- = a_i^+ \sqrt{2S - a_i^+ a_i},$$
$$S_i^z = S - a_i^+ a_i \tag{4}$$

the Hamiltonian is rewritten as

$$H_{eff} \approx -\lambda NS - (J_0(0) - J_2 Z) NS^2 - J_0 S \sum_{i,j} \frac{1}{r_{ij}^p} (a_i a_j^+ + a_i^+ a_j) - JS \sum_{\langle i,j \rangle} (a_i a_j^+ + a_i^+ a_j) + [\lambda + 2S(J_0(0) - JZ)] \sum_i a_i^+ a_i \tag{5}$$

by keeping the bilinear terms only. Here $J_0(0) = \sum_r J_0/r^p$. Z is the coordination number of the nearest neighbors. a_i^+ and a_i denote the creation and annihilation operators of spin deviations, respectively.

After making the Fourier transformations

$$a_l = N^{-\frac{1}{2}} \sum_k e^{ik\cdot l} b_k , a_l^+ = N^{-\frac{1}{2}} \sum_k e^{ik\cdot l} b_k^+ \quad (6)$$

the effective Hamiltonian is computed to be

$$H_{eff} = E_0 + \sum_k \omega_k b_k^+ b_k \quad (7)$$

where

$$E_0 = -\lambda NS - (J_0(0) - JZ)NS^2 \quad (8)$$

and

$$\omega_k = S[J_0(0) - J_0(k)] - S[ZJ - J(k)] + \lambda \quad (9)$$

Here $J_0(k)/J_0(0)$ and $J(k)/(JZ)$ are the structure factors for the long-range and nearest-neighbor interactions, respectively. They are given by

$$J_0(k) = \sum_r \frac{J_0}{r^p} e^{ik\cdot r},\ J(k) = \sum_\delta e^{ik\cdot\delta} \quad (10)$$

In one-dimensional case, $J(k) = 2\cos k$ with $Z=2$; and $J_0(k)$ can be expanded in small k[35-36, 49], i. e.,

$$J_0(0) - J_0(k) \approx \begin{cases} J_0\xi(p-2)k^2, & (p>3) \\ -J_0 k^2 \ln k, & (p=3) \\ J_0 A(p) k^{p-1}, & (1<p<3) \end{cases} \quad (11)$$

with

$$A(p) = \frac{\pi}{\Gamma(P)\sin[\pi(p-1)/2]} \quad (12)$$

in the thermodynamic limit $N\to\infty$. Here $\Gamma(p)$ and $\xi(p)$ denote the gamma function and Riemann's zeta function, respectively.

Taking account of the Bose-Einstein distribution function

$$n_k = \langle b_k^+ b_k \rangle = (e^{\omega_k/T} - 1)^{-1} \quad (13)$$

and inserting it into the thermal average of the Eq. (2), we can get the consistent equation

$$\frac{1}{N}\sum_k \frac{1}{e^{\omega_k/T} - 1} = S \quad (14)$$

Here T stands for the temperature. In the large N thermodynamic limit, the summation in Eq. (14) is replaced by the integral in the first Brillouin zone. The Lagrange multiplier λ is self-consistently determined by Eq. (14). λ given by Eq. (14) is a kind of nonzero chemical potential. Thus, if λ is known, we can obtain the solutions for the thermodynamic properties of the system.

2 Results and discussions

In this section, we will discuss how the FLRI and the ANNI affect the thermodynamic properties (such as the critical temperature, internal energy, specific heat, and susceptibility) of one-dimensional ferromagnetic Heisenberg model. For convenience, the interaction J_0 and the spin S are all set to be $J_0 = 1$ and $S = 1/2$, respectively. The coordination number takes $Z = 2$.

2.1 Lagrange multiplier

In order to obtain the thermodynamic properties, it is important to know the temperature-dependent behavior of the Lagrange multiplier λ. Note that λ can be computed from Eq. (14) which is obtained under the constraint condition of zero magnetization. As pointed out in Ref. [10], the Lagrange multiplier λ has the physical meaning of being treated as the nonzero chemical potential.

Using the consistent Eq. (14), λ is plotted as a function of the temperature T in Fig. 1 for $p=2.2$, 2.5, 3.0, 3.5 at $J=0.1$ in Fig. 1 (a), and for $J=0.1$, 0.5, 0.9 when $p=2.2$ in Fig. 1 (b), respectively. If the ANNI J and the interaction range p are given, it is easily found that λ increases as the temperature T increases. When T and p are given, λ increases with the increasing J. For T fixed, the bigger p or J, the larger λ. The calculation of Eq. (14) at small J shows that λ has the low-temperature behavior of being proportion to $T^{(p-1)/(p-2)}$ for $2<p<3$, and to T^2 for $p>3$.

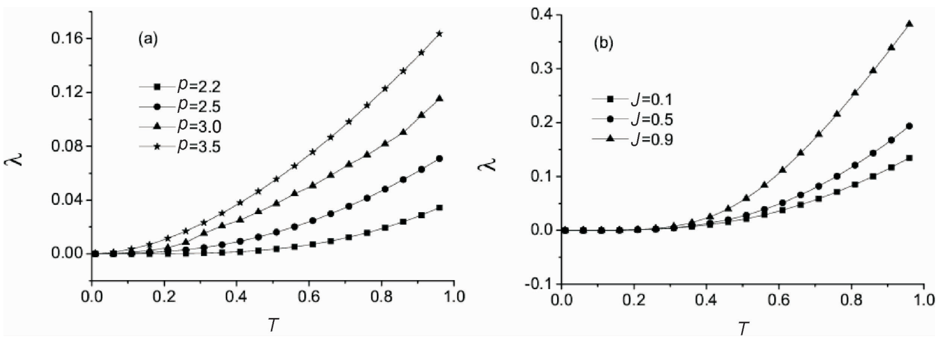

Fig. 1 Temperature dependence of the Lagrange multiplier λ (a) for $p=2.2$, 2.5, 3.0, 3.5 at $J=0.1$, and (b) for $J=0.1$, 0.5, 0.9 when $p=2.2$, respectively

As seen in Fig. 1 (a), λ obtained at the smaller p decreases more slowly than one obtained at the larger p. It is found in Fig. 1 (b) that at a given p, no matter what the value J takes, λ has the similar decaying behavior when the chain is in the low-temperature region of $T<0.2$.

2.2 Critical temperature

In the former section, we have discussed the low-temperature behavior of the nonzero λ. It is interesting that what happens when λ becomes zero at the finite temperature.

Seen from Eqs. (3) and (14), $\lambda=0$ shows that the systems can keep the zero-magnetization condition without needing to introduce the Lagrange multiplier λ in the Hamiltonian (1). This means that the system has a ferromagnetic-paramagnetic phase transition at some finite temperature T_c, which is the critical temperature of the system. Below $T<T_c$, the occurrence of spontaneous magnetization is found. The critical temperature T_c is determined by Eq. (14) for $\lambda=0$,

$$\frac{1}{N}\sum_k \frac{1}{e^{\omega_k^c/T_c}-1}=S \tag{15}$$

with

$$\omega_k^c=S[J_0(0)-J_0(k)]-S[ZJ-J(k)] \tag{16}$$

In the large N thermodynamic limit, Eq. (15) becomes the integral:

$$\frac{1}{2\pi}\int_{1BZ}\frac{dk}{e^{\omega_k^c/T_c}-1}=S \tag{17}$$

where $1BZ$ denotes the first Brillouin zone in one dimension. The calculations of Eq. (17) display that the finite-temperature phase transition exists at $T=T_c\neq 0$ when $1<p<2$. But for $p\geqslant 2$ no transitions exist at any finite temperature $T>0$ with $T_c=0$. This finding agrees with the extended Mermin-Wagner theorem[50] which is developed from the usual Mermin-Wagner theorem[9]. In the case without the ANNI, our T_c obtained in Eq. (17) recovers the one-dimensional results[35].

To obtain the influence of the interaction range p and the ANNI J in the behavior of the critical temperature T_c, Eq. (17) is used to plot the critical temperature T_c as a function of p and J in Fig. 2.

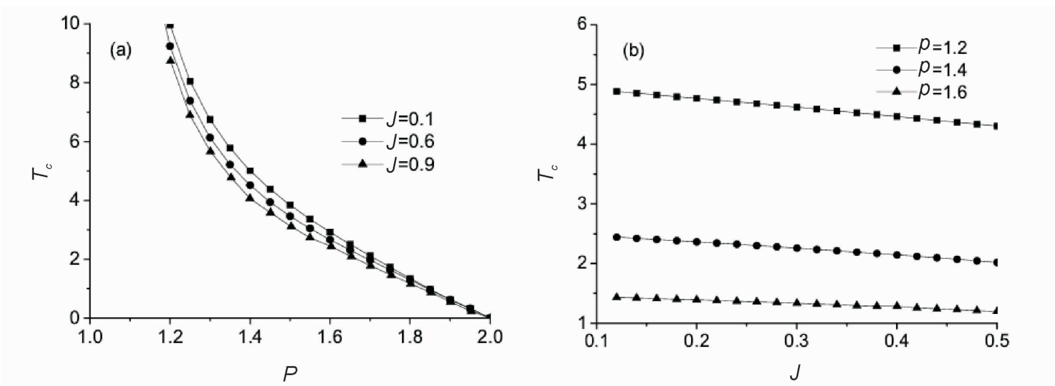

Fig. 2　The critical temperature T_c plotted as a function (a) of the interaction range p for $J=0.1, 0.6, 0.8$, and (b) of the ANNI J for $p=1.2, 1.4, 1.6$, respectively

For $1<p<2$, it can be seen from Fig. 2 that the range parameter p or the ANNI J play the similar poles in the behavior of T_c. As p or J increases, the critical temperature T_c is the decreasing function. This can be explained by that the larger p relaxes the suppression of the thermal fluctuation by the FLRI, and J has a tendency to promote the fluctuations. As a result, both p and J spoil the long-range ferromagnetic ordering in the finite-temperature region, which gives rise to T_c decreasing.

It is interesting that what happens for the critical temperature T_c when the ANNI J is changed to the ferromagnetic next-neighbor interaction $-J$. In this situation, in the region $1<p<2$ the ferromagnetic next-neighbor interaction helps the increase of T_c, which differs from the ANNI does. While the range parameter p still impedes the growth of T_c. For $p=3$, the critical temperature is computed to be $T_c=0$, which agrees with the result[37] obtained in Heisenberg ferromagnetic chains with long-range dipolar forces.

It is shown in Ref. [38] that the continuous $U(1)$ symmetry in the ferromagnetic chain is spontaneously broken for the FLRI in the region $p<p_c$ with a critical value $p_c\leqslant 3$. However, the expression of p_c is not solved in Ref. [38]. In this paper, the critical value $p_c=2$ obtained by the modified spin wave theory, displays that the ferromagnetic long-range

order survives in the region $1 < p < 2$ at finite temperatures $T < T_c$.

2.3 Internal energy

Now, let us consider the behavior of the internal energy U, which is defined by $U = \langle H_{eff} \rangle / N$. From Eq. (7), U is computed to be

$$U = S[2ZJS - J_0\xi(P)S - \lambda] + \frac{1}{N}\sum_k \omega_k n_k \quad (18)$$

in one dimension.

In Fig. 3, the temperature dependence of the internal energy U is presented for the $S = 1/2$ chain at $J = 0.1$ for $p = 2.2$, 2.5, 2.8, and $p = 3.2$, 3.5, 3.8, respectively.

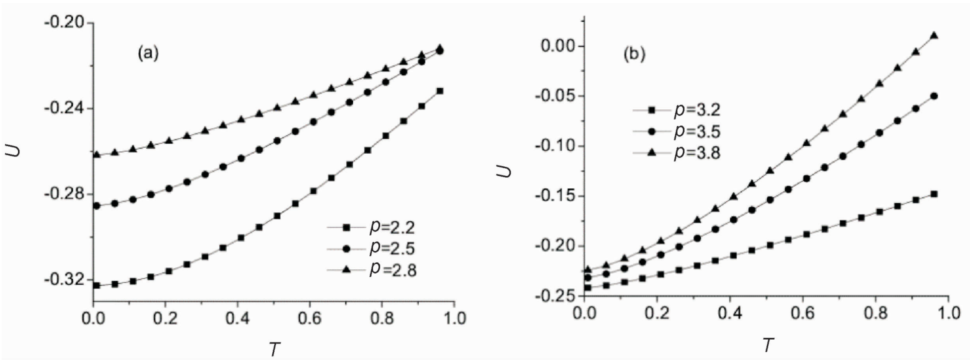

Fig. 3 Temperature dependence of internal energy U at $J = 0.1$ for (a) $p = 2.2$, 2.5, 2.8, and (b) $p = 3.2$, 3.5, 3.8, respectively

From the figures, for $p > 2$ in the disorder phase, we can see that U is the increasing function of both T and p for J given. The main reason for this phenomenon of U increasing with the temperature is that as p increases, the FLRI becomes weak, but the thermal fluctuations get stronger. It is noticed that the effect of the interaction range p on the temperature dependence of U for $2 < p < 3$ is different from that for $p > 3$. Fig. 3(a) shows that the increasing value in p induces the slow growth of U in the region of $2 < p < 3$. While for $p > 3$, the larger p results in the rapid growth of U in the region of low temperature, as seen in Fig. 3(b).

Fig. 4 illustrates that the temperature-dependent behavior of the internal energy U affected by the ANNI J.

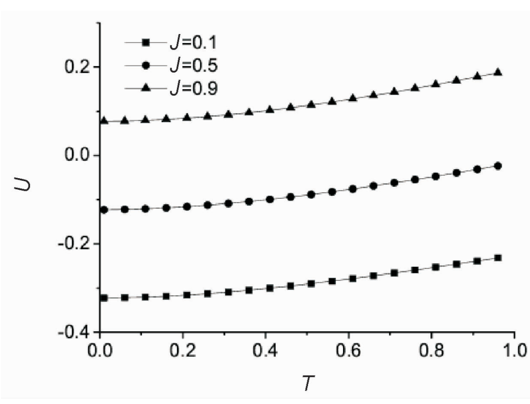

Fig. 4 Temperature dependence of internal energy U for $J = 0.1$, 0.5, 0.9 when $p = 2.2$

When both the temperature and the interaction range are given, the internal energy U is on the increase as the ANNI J goes up. This behavior induced by the ANNI causing harm to the stability of the long-range ferromagnetic ordering at the finite temperatures.

2.4 Heat capacity

In this section, we will study how the FLRI and ANNI affect the temperature-dependent behavior of the specific heat $C = \partial U / \partial T$. By mean of Eq. (18), one has

$$C = -S\frac{\partial\lambda}{\partial T} + \frac{1}{N}\sum_k n_k \frac{\partial\lambda}{\partial T} - \frac{1}{N}\sum_k \omega_k n_k (n_k + 1)\left(\frac{1}{T}\frac{\partial\lambda}{\partial T} - \frac{\omega_k}{T^2}\right) \quad (19)$$

Here $\frac{\partial\mu}{\partial T}$, which can be obtained from the self-consistent Eq. (14), is given by

$$\frac{\partial\mu}{\partial T} = \frac{1}{T}\frac{\sum_k \omega_k n_k (n_k + 1)}{\sum_k n_k (n_k + 1)} \quad (20)$$

In the low-temperature region, we employ Eqs. (19) and (20) to obtain the temperature dependence of the specific heat C, as shown in Fig. 5.

The specific heat C exhibits the peak phenomenon which is characteristic of the interaction range p and the ANNI J in the low-temperature region. Fig. 5(a) shows that the specific heat C starts from zero, and increases with the temperature, arrives at its maximum in the low-temperature region. As p decreases, the maximum height of the specific heat increases, and its maximum width is widening, and the corresponding maximum position moves to the higher temperature. If p is fixed, the large J helps the increase of the specific heat and its maximum height.

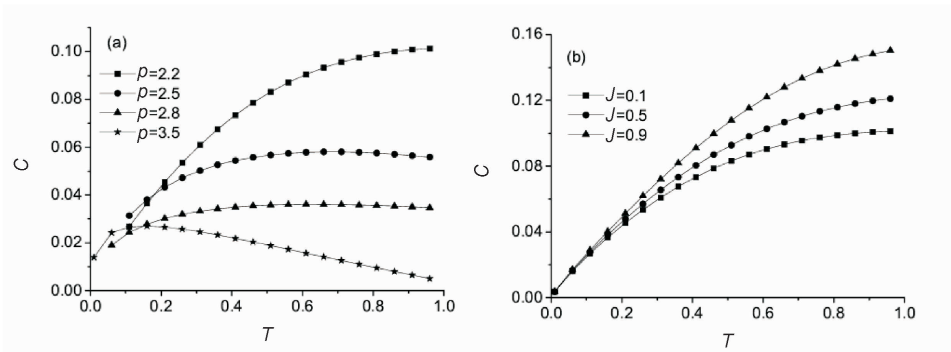

Fig. 5　Temperature dependence of the specific heat capacity C for (a) $p = 2.2$, 2.5, 2.8, 3.5 at $J = 0.1$, and (b) $J = 0.1$, 0.5, 0.9 at $p = 2.2$, respectively.

At low temperatures and the small ANNI, the spin-wave calculations give the specific heat C to be in the form of $T^{1/(p-1)}$ for $2 < p < 3$ and $T^{1/2}$ for $p > 3$, respectively. Then the quantities $C/T^{1/(p-1)}$ and $C/T^{1/2}$ are considered as the coefficients of the specific heat at low temperatures for $2 < p < 3$ and $p > 3$, and their temperature dependences are shown in Fig. 6 and Fig. 7, respectively.

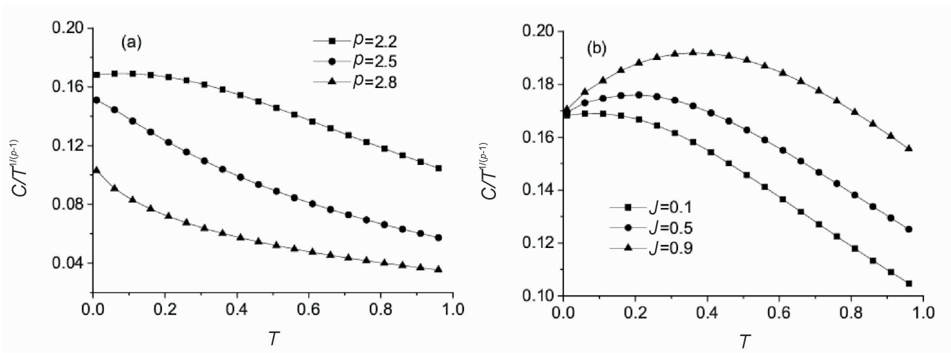

Fig. 6　Temperature dependence of $C/T^{1/(p-1)}$ for (a) $p = 2.2$, 2.5, 2.8 at $J = 0.1$, and (b) $J = 0.1$, 0.5, 0.9 at $p = 2.2$, respectively.

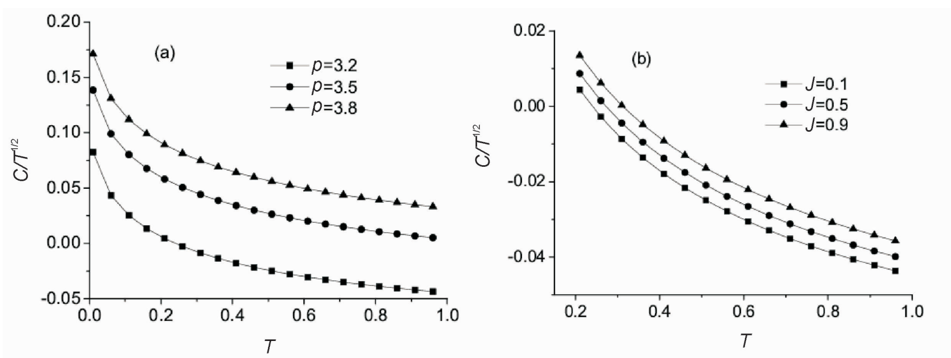

Fig. 7　Temperature dependence of $C/T^{1/2}$ for (a) $p = 3.2$, 3.5, 3.8 at $J = 0.1$, and (b) $J = 0.1$, 0.5, 0.9 at $p = 3.2$, respectively

When p is not far away from $p = 2$ in the region of $p > 2$, the coefficient $C/T^{1/(p-1)}$ displays the maximum behavior at low temperatures. Its maximum becomes larger and more widens with increasing J, and shifts to the higher temperature. However, if the large p is far from $p = 2$, this kind of the maximum behavior disappears, and $C/T^{1/(p-1)}$ decreases as the temperature increases. Unlike the behavior of $C/T^{1/(p-1)}$ for $2<p<3$, $C/T^{1/2}$ is only the decreasing functions of the temperature T in the region of $p>3$ and $0\leqslant J\leqslant 1$. For the given T, it is shown that both p and J give the helping hands to the growth of $C/T^{1/2}$.

In the zero-temperature limit, the values of $C/T^{1/(p-1)}$ is the decreasing (or increasing) function of p (or J). For example, the zero-temperature values of $C/T^{1/(p-1)}$ are computed to be 0.168 313, 0.169 393, 0.170 503 for $J=0.1$, 0.5, 0.9 at $p=2.2$, respectively. For $J=0$ and $p=2.2$, $\lim_{T\to 0} C/T^{1/(p-1)}=0.166\ 91$ which agrees with the result obtained in Ref. [35]. As shown in Fig. 7, the zero-temperature values of $C/T^{1/2}$ are the increasing function of both p and J.

In the nearest-neighbor limit $p\to\infty$, the FLRI is reduced to the ferromagnetic nearest-neighbor interaction, and then the model discussed in this paper becomes the Heisenberg chain with the ferromagnetic and antiferromagnetic nearest-neighbor interactions. In this case, for $J=0$ and $S=1/2$, the analytical calculation within the modified spin wave theory gives the zero-temperature value of the specific heat coefficient to be $\lim_{T\to 0} C/T^{1/2}=0.781\ 64$, which recovers the result obtained by the Takahashi's scheme[10], and agrees very well with the BA value 0.781 5[51].

The analysis and discussion above are for the low-temperature behavior of the specific heat C in the region $p>2$, where the system is in the paramagnetic phase for $T>0$ with the critical temperature $T_c=0$. However, in the region $1<p<2$, there exists the spontaneous magnetization at temperatures $T<T_c$ with $T_c>0$. In this paper, we are interested in the specific heat C at low temperatures $T<T_c$, where C is given by $C=\frac{1}{N}\sum_k \omega_k^2 T^{-2} n_k(n_k+1)$ within the spin wave theory for $1<p<2$. It is found that the low-temperature behavior of C in the region $1<p<2$ is similar to that in the region $2<p<3$.

2.5 Magnetic susceptibility

In the following, we turn to consider the behavior of the magnetic susceptibility χ, which is defined by

$$\chi=\frac{1}{T}\sum_r \langle S_0^z S_r^z\rangle \tag{21}$$

Due to the absence of the applied magnetic field in Eq. (1), the system has the spin-rotational symmetry, which results in the spin-correlation functions

$$\langle S_0^x S_r^x\rangle=\langle S_0^y S_r^y\rangle=\langle S_0^z S_r^z\rangle.$$

Then the susceptibility χ is uniform, and it is rewritten as

$$\chi=\frac{1}{3T}\sum_r (\langle S_0^x S_r^x\rangle+\langle S_0^y S_r^y\rangle+\langle S_0^z S_r^z\rangle) \tag{22}$$

With the help of Holstein-Primakoff and Fourier transformations, the susceptibility χ is computed to be

$$\chi=\frac{1}{3TN}\sum_k n_k(n_k+1) \tag{23}$$

In the regime of the very low temperature, the susceptibility χ can be solved from Eq. (23) at the small ANNI J. The susceptibility χ behaves as $T^{-(p-1)/(p-2)}$ for $2<p<3$ and T^{-2} for $p>3$ at low temperatures, respectively. Then like in the low-temperature case of the specific heat C, the quantities $\chi T^{(p-1)/(p-2)}$ and χT^2 are defined as the coefficients of the susceptibility at low temperatures for $2<p<3$ and $p>3$, respectively.

Temperature dependence of the susceptibility and its coefficients are plotted in Figs. 8 ~ Figs. 10 for some selected values of p and J, respectively. Fig. 8 shows that the susceptibility χ is a decreasing function of the temperature. However, the susceptibility coefficient $\chi T^{(p-1)/(p-2)}$ is the increasing function of the temperature for both $2<p<3$ and $p>3$, as seen in Fig. 9. It is found in Fig. 10 that at low temperatures, the susceptibility coefficient χT^2 shows the intriguing behavior in the region of $p>3$. At very low temperature $T<0.2$, χT^2 displays a minimum. As the temperature increases, χT^2 firstly decreases, and then increases after passing through the minimum.

The interaction range p affects the temperature-dependent behaviors of the susceptibility and its coefficients in a similar way to the ANNI J. If the temperature T is fixed, the large J and the large p both impede the increase of the susceptibility, while the susceptibility coefficients $\chi T^{(p-1)/(p-2)}$ and χT^2 both increase as p or J increases. Fig. 8(a) shows that the interaction range causes the stronger suppression of the susceptibility for $p>3$ than for $2<p<3$. In Fig. 8(b), the influences of the ANNI in the susceptibility χ is weak in the region of small p and J, and so does the susceptibility coefficient $\chi T^{(p-1)/(p-2)}$ in Fig. 9(b). It is shown in Fig. 9(a) that the smaller p induces the susceptibility coefficient to rise slowly. The height of the minimum of χT^2 increases with the increase of both p and J, as shown in Fig. 10(a) and Fig. 10(b).

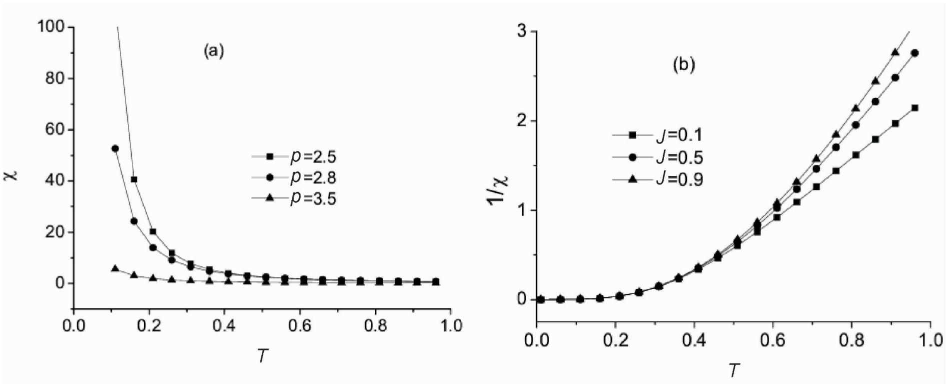

Fig. 8　Temperature dependence of susceptibility χ for (a) $p = 2.5$, 2.8, 3.5 at $J = 0.1$, and (b) $J = 0.1$, 0.5, 0.9 at $p = 2.2$, respectively

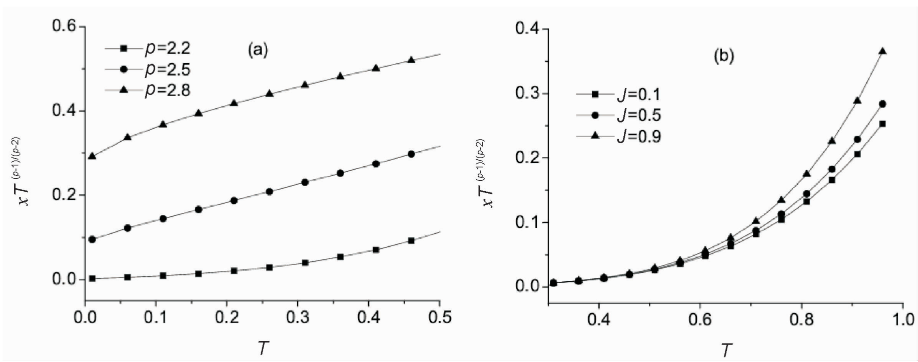

Fig. 9　Temperature dependence of $\chi T^{(p-1)/(p-2)}$ for (a) $p = 2.2$, 2.5, 2.8 at $J = 0.1$, and (b) $J = 0.1$, 0.5, 0.9 at $p = 2.2$, respectively

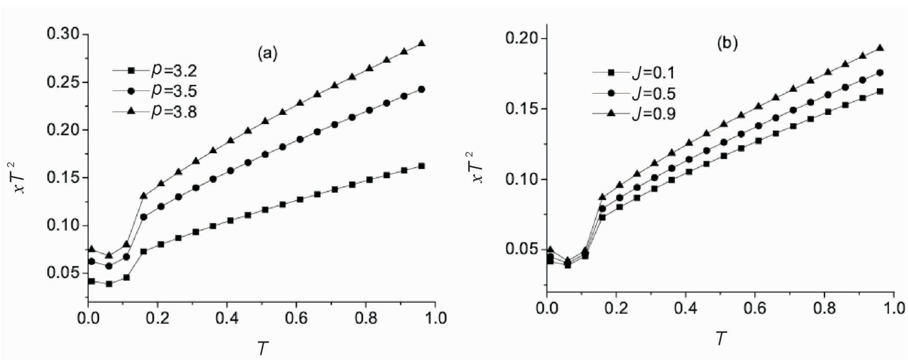

Fig. 10　Temperature dependence of χT^2 for $p = 3.2$, 3.5, 3.8 at $J = 0.1$, and (b) $J = 0.1$, 0.5, 0.9 at $p = 3.2$, respectively

Note that in the zero-temperature limit, the values of the susceptibility coefficients $\lim_{T\to 0} \chi T^{(p-1)/(p-2)}$ and $\lim_{T\to 0} \chi T^2$ all increase with the increase in p or J, as shown in Fig. 9 and Fig. 10. At $p = 2.2$, $\lim_{T\to 0} \chi T^{(p-1)/(p-2)} = 0.000\,153$, $0.002\,977$ for $J = 0$, 0.1, respectively. This value 0.000 153 is just the result in the case without the ANNI[35]. For $J = 0$ and $p \to \infty$, our $\lim_{T\to 0} \chi T^2 = 1/24$, which is obtained by the self-consistent method, reproduces the result obtained by Takahashi's scheme[10]. It is also in good agreement with the BA value 0.041 675[51], and with 0.041 667 obtained by Green's function method[52-53] and the quantum Monte Carlo[53].

3　Conclusion

In this paper, with the help of Takahashi's idea constraining the total magnetization to be zero, the modified spin-wave theory has been applied to the ferromagnetic Heinsenberg chain with the FLRI and the ANNI. It is found that the FLRI range p and the ANNI J have great influence on the low-temperature properties of the system. For $J = 0$, our results agree well with the exact BA results and the quantum Monte Carlo data.

The internal energy U as well as the chemical potential λ is the increasing functions of both p and J. But the magnetic susceptibility χ and the temperature T_c decreases with the increase in p or J. At the very low temperatures and the small J, the specific heat C and susceptibility χ display the power laws in temperature T: $C \sim T^{1/(p-1)}$ and $\chi \sim T^{(p-1)/(p-2)}$ for $2<p<3$, and $C \sim T^{1/2}$ and $\chi \sim T^{-2}$ for $p>3$, respectively.

At low temperatures, it is found that the specific heat C exhibits the temperature-dependent peak behavior, along with the specific heat coefficient $C/T^{1/(p-1)}$; while the susceptibility coefficient χT^2 shows a minimum. As p increases, the maximum of C shortens and narrows, and its position shifts to the lower temperature. Note that J promotes the growth of C. When p is close to $p=2$, the coefficient $C/T^{1/(p-1)}$ has the maximum which grows up and widens with increasing J, and shifts to the higher temperature. However, for the large p the maximum behavior of $C/T^{1/(p-1)}$ can't survive. For $p>3$, as the temperature increases, the susceptibility coefficient χT^2 firstly decreases, and then increases after passing through the minimum whose height increases with the increase of both p and J.

References:

[1] Anderson P W. An approximate quantum theory of the antiferromagnetic ground state[J]. Physical Review, 1952, 86(5): 694-701.

[2] Kubo R. The spin-wave theory of antiferromagnetics[J]. Physical Review, 1952, 87(4): 568-580.

[3] Oguchi T. Theory of spin-wave interactions in ferro- and antiferromagnetism[J]. Physical Review, 1960, 117(1): 117-122.

[4] Kreisel A, Peter M, Kopietz P. Singular spin-wave theory and scattering continua in the cone state of Cs_2CuCl_4[J]. Physical Review B, 2014, doi: 10.1103/PhysRevB.90.075130.

[5] Ishizuka H, Balents L. Magnetism in $S=1/2$ double perovskites with strong spin-orbit interactions[J]. Physical Review B, 2014, doi:10.1103/PhysRevB.99.184422.

[6] Correggi M, Giuliani A, Seiringer R. Validity of spin-wave theory for the quantum Heisenberg model[J]. Europhysics Letters, 2014, doi: 10.1209/0295-5075/108/20003.

[7] Toth S, Lake B. Linear spin wave theory for single-Q incommensurate magnetic structures[J]. Journal of Physics: Condensed Matter, 2015, doi: 10.1088/0953-8984/27/16/166002.

[8] Chisnell R, Helton J S, Freedman D E, et al. Topological magnon bands in a kagome lattice ferromagnet[J]. Physical Review Letters, 2015, doi: 10.1103/PhysRevLett.115.147201.

[9] Mermin N D, Wagner H. Absence of ferromagnetism or antiferromagnetism in one- or two-dimensional isotropic Heisenberg models[J]. Physical Review Letters, 1966, 17(22):1133-1136.

[10] Takahashi M. Few-dimensional Heisenberg ferromagnets at low temperature[J]. Physical Review Letters, 1987, 58(2): 168-170.

[11] Takahashi M. Modified spin-wave theory of a square-lattice antiferromagnet[J]. Physical Review B, 1989, 40(4): 2494-2501.

[12] Hirsch J E, Tang S. Spin-wave theory of the quantum antiferromagnet with unbroken sublattice symmetry[J]. Physical Review B, 1989, 40(7): 4769- 4771.

[13] Chen Y, Wu Y. The low-temperature properties of the spin-one Heisenberg antiferromagnetic chain with the single-ion anisotropy[J]. Solid State Communications, 2013, 159: 49-54.

[14] Yamamoto S, Noriki Y. Spin-wave thermodynamics of square-lattice antiferromagnets revisited[J]. Physical Review B, 2019, doi: 10.1103/PhysRevB.99.094412.

[15] Yamamoto S. Bosonic representation of one-dimensional Heisenberg ferrimagnets[J]. Physical Review B, 2004, doi:10.1103/PhysRevB.69.064426.

[16] Karchev N. Towards the theory of ferrimagnetism[J]. Journal of Physics: Condensed Matter, 2008, doi: 10.1088/0953-8984/20/32/325219.

[17] Karchev N. Towards the theory of ferrimagnetism: II[J]. Journal of Physics: Condensed Matter, 2009, doi: 10.1088/0953-8984/21/21/216003.

[18] Silva W M D, Montenegro-Filho R R. Magnetic-field-temperature phase diagram of alternating ferrimagnetic chains: Spin-

wave theory from a fully polarized vacuum[J]. Physical Review B, 2017, doi:10.1103/PhysRevB.96.214419.
[19] Su G, Xing H Z, Wang J B, et al. Specific heat of spinone-half frustrated Heisenberg ladder[J]. Physics Letters A, 2001, 283(3/4): 249-256.
[20] Rocha-Filho G M, Pires A S T, Gouvêa M E. Modified spin-wave theory for the $S=1$ frustrated antiferromagnetic Heisenberg chain[J]. The European Physical Journal B, 2007, 56(1): 7-14.
[21] Hida K, Iino T. Modified spin wave analysis of low temperature properties of the spin-1/2 frustrated ferromagnetic ladder [J]. Journal of the Physical Society of Japan, 2012, doi:10.1143/JPSJ.81.034708.
[22] Laflorencie N, Luitz D J, Alet F. Spin-wave approach for entanglement entropies of the J_1-J_2 Heisenberg antiferromagnet on the square lattice[J]. Physical Review B, 2015, doi: 10.1103/PhysRevB.92.115126.
[23] Ghorbani E, Shahbazi F, Mosadeq H. Quantum phase diagram of distorted J_1-J_2 Heisenberg $S=1/2$ antiferromagnet in honeycomb lattice: A modified spin wave study[J]. Journal of Physics: Condensed Matter, 2016, doi: 10.1088/0953-8984/28/40/406001.
[24] Hauke P, Roscilde T, Murg V, et al. Modified spin-wave theory with ordering vector optimization: Frustrated bosons on the spatially anisotropic triangular lattice[J]. New Journal of Physics, 2010, doi: 10.1088/1367-2630/12/5/053036.
[25] Liao L, Chen Y. Spin-wave theory applied to the low-temperature properties of the spin-1/2 ferromagnetic chain with the y-direction exchange anisotropy[J]. Superlattices and Microstructures, 2014, 73(1): 82-97.
[26] Liao Y, Chen Y, Chen J P, et al. Modified spin-wave theory applied to one-dimensional Heisenberg ferromagnet with the nearestneighbor and next-nearest-neighbor exchange anisotropies[J]. International Journal of Modern Physics B, 2019, doi: 10.1142/S0217979219501066.
[27] Gouvêa M E, Pires A S T. Effect of spin-phonon coupling on the Haldane gap in antiferromagnetic Heisenberg chains[J]. Physical Review B, 2007, doi:10.1103/PhysRevB.75.052401.
[28] Malard M, Pires A S T. Influence of magnon-phonon coupling on the phonon dynamics of one-dimensional antiferromagnets [J]. Physical Review B, 2007, doi:10.1103/PhysRevB.76.104407.
[29] Lima L S. Spin transport of the quantum integer spin S one-dimensional Heisenberg antiferromagnet coupled to phonons[J]. The European Physical Journal B, 2013, 86(3): 99.
[30] Hauke P. Quantum disorder in the spatially completely anisotropic triangular lattice[J]. Physical Review B, 2013, doi: 10.1140/epjb/e2013-30924-7.
[31] Celi A, Grass T, Ferris A J, et al. Modified spin-wave theory and spin-liquid behavior of cold bosons on an inhomogeneous triangular lattice[J]. Physical Review B, 2016, doi:10.1103/PhysRevB.94.075110.
[32] Yamamoto S, Nakanishi T. Spin-wave description of nuclear spin-lattice relaxation in $Mn_{12}O_{12}$ acetate[J]. Physical Review Letters, 2002, doi: 10.1103/PhysRevLett.89.157603.
[33] Hori H, Yamamoto S. Nuclear magnetic relaxation in the ferrimagnetic chain compound $NiCu(C_7H_6N_2O_6)(H_2O)_3 \cdot 2H_2O$: Three-magnon scattering? [J]. Journal of Physics: Condensed Matter, 2004, 16(49): 9023-9029.
[34] Dmitriev D V, Krivnov V Y, Richter J, et al. Thermodynamics of a delta chain with ferromagnetic and antiferromagnetic interactions[J]. Physical Review B, 2019, doi:10.1103/PhysRevB.99.094410.
[35] Nakamo H, Takahashi M. Quantum Heisenberg model with long-range ferromagnetic interactions[J]. Physical Review B, 1994, 50(14): 10331-10334.
[36] Nakamo H, Takahashi M. Magnetic properties of quantum Heisenberg ferromagnets with long-range interactions[J]. Physical Review B, 1995, 52(9): 6602-6610.
[37] Isidori A, Ruppel A, Kreisel A, et al. Quantum criticality of dipolar spin chains[J]. Physical Review B, 2011, doi:. 10.1103/PhysRevB.84.184417.
[38] Maghrebi M F, Gong Z X, Gorshkov A V. Continuous symmetry breaking in 1D long-range interacting quantum systems [J]. Physical Review Letters, 2017, doi:10.1103/physrevlett.119.023001.
[39] Sandvik A W. Ground states of a frustrated quantum spin chain with long-range interactions[J]. Physical Review Letters, 2010, doi,10.1103/PhysRevLett.104.137204.
[40] Bravo B, Cabra D C, Albarracín F A G, et al. Long-range interactions in antiferromagnetic quantum spin chains[J]. Physical Review B, 2017, doi:10.1103/PhysRevB.96.054441.
[41] Pramanik A K, Banerjee A. Critical behavior at paramagnetic to ferromagnetic phase transition in $Pr_{0.5}Sr_{0.5}MnO_3$: A bulk magnetization study[J]. Physical Review B, 2009, doi:10.1103/physrevb.79.214426.

[42] Zhang L, Fang J, Fan J Y, et al. Critical behavior of the half-doped perovskite $Pr_{0.5}Sr_{0.5}CoO_{3-\Delta}$[J]. Journal of Alloys and Compounds, 2014, 588: 294-299.
[43] Madhogaria R P, Clements E M, Kalappattil V, et al. Metamagnetism and kinetic arrest in a long-range ferromagnetically ordered multicaloric double perovskite Y_2CoMnO_6[J]. Journal of Magnetism and Magnetic Materials, 2020, doi: 10.1016/j.jmmm.2020.166821.
[44] Nolting W, Ramakanth A. Quantum theory of magnetism[M]. Berlin: Springer, 2009.
[45] Porras D, Cirac J I. Effective quantum spin systems with ion traps[J]. Physical Review Letters, 2004, doi: 10.1103/PhysRevLett.92.207901.
[46] Kim K, Chang M S, Islam R, et al. Entanglement and tunable spin-spin couplings between trapped ions using multiple transverse modes[J]. Physical Review Letters, 2009, doi: 10.1103/PhysRevLett.103.120502.
[47] Neyenhuis B, Zhang J, Hess P W, et al. Observation of prethermalization in long-range interacting spin chains[J]. Science Advances, 2017, doi: 10.1126/sciadv.1700672.
[48] Holstein J, Primakoff N. Field dependence of the intrinsic domain magnetization of a ferromagnet[J]. Physical Review, 1940, 58(15): 1098-1113.
[49] Sousa J R D, Branco N S. Two-dimensional quantum spin-1/2 Heisenberg model with competing interactions[J]. Physical Review B, 2005, doi: 10.1103/PhysRevB.72.134421.
[50] Bruno P. Absence of spontaneous magnetic order at nonzero temperature in one- and two-dimensional Heisenberg and XY systems with long-range interactions[J]. Physical Review Letters, 2001, doi: 10.1103/PhysRevLett.87.137203.
[51] Yamada M, Takahashi M. Critical behavior of spin-1/2 one-dimensional Heisenberg ferromagnet at low temperatures[J]. Journal of the Physical Society of Japan, 1986, 55(6): 2024-2036.
[52] Antsygina T N, Poltavskaya M I, Poltavsky I I, et al. Thermodynamics of low-dimensional spin-1/2 Heisenberg ferromagnets in an external magnetic field within a green function formalism[J]. Physical Review B, 2008, doi: 10.1103/PhysRevB.77.024407.
[53] Junger I J, Ihle D, Bogacz L, et al. Thermodynamics of Heisenberg ferromagnets with arbitrary spin in a magnetic field[J]. Physical Review B, 2008, doi: 10.1103/PhysRevB.77.174411.

【责任编辑: 卓祯雨】

(上接第47页)

[18] LeSage J, Pace R K. Introduction to spatial econometrics[M]. New York: CRC Press, 2009: 33-41.
[19] 聂辉华. 从政企合谋到政企合作——一个初步的动态政企关系分析框架[J]. 学术月刊, 2020, 52(6): 44-56.
[20] 许志端, 阮舟一龙. 营商环境、技术创新和企业绩效——基于我国省级层面的经验证据[J]. 厦门大学学报(哲学社会科学版), 2019(5): 123-134.
[21] 沈弋, 徐光华, 钱明. 慈善捐赠、研发投入与财务资源的调节作用——基于战略间互动视角[J]. 管理评论, 2018, 30(2): 159-171.
[22] Friedman M. The social responsibility of business is to increase its profits[J]. New York Times Magazine, 1970, 9(13): 122-126.
[23] Becker-Olsena K L, Cudmoreb B A, Hill R P. The impact of perceived corporate social responsibility on consumer behavior[J]. Journal of Business Research, 2006, 59(1): 46-53.
[24] 权小锋, 吴世农, 尹洪英. 企业社会责任与股价崩盘风险:"价值利器"或"自利工具"?[J]. 经济研究, 2015, 50(11): 49-64.
[25] 贾建林, 樊霞. 基于对外研发创新过程的企业创新持续性实现机制研究[J]. 中国科技论坛, 2021(11): 78-87.
[26] Suárez D. Persistence of innovation in unstable environments: Continuity and change in the firm's innovative behavior[J]. Research Policy, 2014, 43(4): 726-736.
[27] 王睿智, 冯永春, 许晖. 声誉资源和关系资源对突破式创新影响关系[J]. 管理科学, 2017, 30(5): 87-101.
[28] 唐擎. 企业社会责任对团队创新绩效的影响机制研究[D]. 北京: 中央财经大学, 2019.
[29] 张雪, 韦鸿. 企业社会责任、技术创新与企业绩效[J]. 统计与决策, 2021, 37(5): 157-161.

【责任编辑: 周 全】